Desalination 495 (2020) 114667

Contents lists available at ScienceDirect

Desalination

journal homepage: www.elsevier.com/locate/desal

Construction of ionic thermo-responsive PNIPAM/γ-PGA/PEG hydrogel as a draw agent for enhanced forward-osmosis desalination

Keyuan Zhang, Fei Li, Yan Wu, Li Feng*, Liqiu Zhang

College of Environmental Science and Engineering, Beijing Forestry University, Beijing 100083, China

GRAPHICAL ABSTRACT

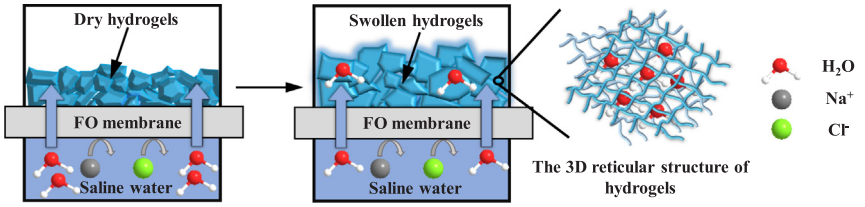

ARTICLE INFO

Keywords:
Ionic thermo-responsive hydrogel
Response surface methodology
Draw agent
Dewatering
Forward osmosis

ABSTRACT

To achieve efficient forward osmosis (FO) for desalination, thermal-responsive hydrogels were synthesized by polymerization of N-isopropylacrylamide (NIPAM) in the presence of ionic polyglutamic acid (γ-PGA) and pore-forming polyethylene glycol (PEG). The equilibrium swelling ratio (ESR) and deswelling behaviour of PNIPAM/γ-PGA/PEG hydrogels were investigated at a series of dosages of reactants (γ-PGA, PEG, initiator and cross-linker). The PNIPAM/γ-PGA/PEG hydrogel revealed effective deswelling response at low temperature (35.20 °C). The highest ESR was 94.76 g/g, and the fastest dewatering ratio could reach 97.64% within 30 min. The optimal mass ratio of comonomers (NIPAM, γ-PGA and PEG), crosslinker and initiator was fixed at 1:0.2:1:0.01:0.01 determined by the response surface method (RSM). It was also found by RSM that the ESR was significantly dependent on cross-linker and the interaction between initiator and γ-PGA. The optimal hydrogel was examined as draw agent, employing deionized (DI) water and 0.05, 0.1 and 0.2 wt% NaCl solution as the feed, which showed the enhanced water fluxes at 1.99, 1.65, 1.31 and 1.08 LMH in initial 0.5 h. In addition, the hydrogel showed promising recyclability in term of water flux in three cycles.

1. Introduction

As an emerging technology, forward osmosis (FO) process has garnered enough attention due to the advantages of the lesser energy consumption and lower membrane fouling compared with conventional methods, such as reverse osmosis (RO) [1,2]. In FO process, water molecules permeation occurred spontaneously across a semipermeable membrane due to natural osmotic pressure gradient between feed solute and draw agent [3]. Then, the essential step was water recovery from draw agent for the production of freshwater and the regeneration of the draw agent, which was primary energy demand [4]. The high cost and energy consumption of regeneration restricted draw agent's application in an industrial FO process. For instance, the recovery of the common draw solutes (like salts: NaCl, KCl and $MgCl_2$) required membrane distillation (MD) with the reported energy consumption of ~10 kWh/m^3 [5,6]. Hence, the development of draw agent which could be regenerated with high efficiency at low cost still needed to be promoted.

Of the draw agents explored to date, the thermo-responsive hydrogels synthesized from polymer showed several potential advantages,

* Corresponding author.
E-mail address: fengli_hit@163.com (L. Feng).

https://doi.org/10.1016/j.desal.2020.114667
Received 28 May 2020; Received in revised form 15 July 2020; Accepted 4 August 2020

such as low energy consumption of regeneration, negligible reverse flux in FO and so on [7]. As an excellent thermo-responsive example, poly (N-isopropylacrylamide) (PNIPAM) hydrogel was used to explain work principle of thermo-responsive hydrogel. It underwent a phase transition from swollen (or hydrophilic) state to dewatering (or hydrophobic) state when heated up to its lower critical solution temperature (LCST) [8]. The LCST was resulted from the realignment of water molecules around hydrophobic and hydrophilic group (alkyl and acrylate, respectively) in the polymer chains, causing the collapse of hydrogel network and water release [9]. PNIPAM hydrogel could release ~70% of the entrapped water above 50 °C [10]. To further improved the performance of the hydrogel-driven FO process, a plenty of ionic polymers have been used (or proposed to be used) in PNIPAM-based hydrogel [11]. Li and co-workers demonstrated that the NIPAM-based hydrogels copolymerized with sodium acrylate (SA) significantly enhanced FO flux [12]. Because the strong interaction between ionic groups of SA and water molecules (e.g., hydration and ionization) created a high osmotic pressure. There was accompanying problem that excessive SA hindered the phase transition of NIPAM, leading the compromise on dewatering performance. Similar conclusion has appeared in other previous literatures. The copolymer hydrogel of sodium styrene-4-sulfonate (SSS) and NIPAM did not reveal the thermally responsive dewatering behaviour [13]. Almost no water could be recovered from co-polymer microgels of NIPAM and acrylic acid (P (NIPAM-AA)) with 50% or 70% AA content beyond their LCST [14]. Even so, the water absorption capacity of hydrogel improved significantly as ionic monomer presented. Moreover, the response ability of ionic hydrogel can be even higher if strategically designed their 3D network structure. Li et al. synthesized hydrogels with different SA concentrations in an attempt to retain the LSCT response [12]. Some researchers prepared porous hydrogel with polyethylene glycol (PEG) as pore-generating agent, which greatly improved the water absorption and dewatering performance of hydrogel [15,16]. The porous structure and response performance of hydrogel could be manipulated by the cross-linker and initiator content in composition of hydrogel in drug delivery application [17–19]. Hence, it was possible to further develop the ionic thermo-responsive hydrogel, which maintained the high permeable flux and the excellent LCST for easy dewatering and regeneration.

Herein, polyglutamic acid (γ-PGA) and PEG were selected to copolymerize with NIPAM to synthesize a kind of ionic thermo-responsive hydrogel with porous structure. As an ionic monomer, γ-PGA was added to improve osmotic pressure, which could be linked to other polymer through a cross-link between a α-amino group and an γ-carboxyl group to form ionic hydrogels [20]. PEG acted as a pore-forming agent was expected to be favourable for water transport and then efficiently enhanced water recovery of hydrogel [21]. The effects of the proportion of composition (γ-PGA, PEG, initiator and cross-linker) on equilibrium swelling ratio (ESR) and deswelling behaviours of PNIPAM/γ-PGA/PEG hydrogels were systematically investigated to optimize structure of the hydrogel. Moreover, owing to the limitation of a single-factor experiment, the interactive influences of variables (initiator, cross-linker and γ-PGA) on ESR of hydrogel were explored by response surface methodology (RSM). The optimal preparation scheme of PNIPAM/γ-PGA/PEG hydrogel was obtained. Then, the water flux and recycle performance of the optimum PNIPAM/γ-PGA/PEG hydrogel were evaluated in detail in FO process.

2. Materials and methods

2.1. Materials

NIPAM (≥99%, AR) was purchased from J&K, China. γ-PGA (92%, AR) and PEG (Mn: 10,000 g/mol) were purchased from MERCK, Germany. The cross-linker *N*, *N*′-methylenebisacrylamide (MBA, 99%) was obtained from Xiya Reagent, China. The initiator ammonium persulfate (APS, ≥98%) and the accelerant *N*, *N*, *N*, *N*′-tetramethylethanoldiamine (TEMED, > 99%) were purchased from AMRESCO, US. Sodium chloride (NaCl, > 99.5%) and potassium bromide (KBr, > 99.7%) were purchased from Beijing Chemical Works, China. Cellulose triacetate (CTA) membranes with a nested polyester screen mesh were purchased from Hydration Technologies Inc. (HTI, USA).

2.2. Synthesis of the PNIPAM/γ-PGA/PEG hydrogels

NIPAM (1.0000 g), γ-PGA and PEG monomers were dissolved in deionized (DI) water (15 mL) to form comonomer solutions. The MBA cross-linker was added to these solutions, which were mixed by ultrasonication at room temperature for 30 min. The resultant solutions were deaerated by bubbling with nitrogen for 25 min. Then, the APS initiator and TEMED accelerant (40 μL) were immediately added to the above solutions. The polymerization was carried out for 2 h under sealed conditions to form the hydrogels. To remove the unreacted monomers, the obtained hydrogels were cut into small pieces and immersed in DI water for 5 days. The DI water was changed every 6–8 h to ensure the complete removal of the unreacted monomers. Then, the hydrogels were dried at 80 °C in an oven and stored in a desiccator [22]. During hydrogel preparation, the dosages of reactants (γ-PGA, PEG, initiator and cross-linker) were changed to obtain a series of PNIPAM/γ-PGA/PEG hydrogels (Table 1).

2.3. Characterization of the PNIPAM/γ-PGA/PEG hydrogels

Fourier transform infrared spectra (FT-IR, VERTEX 70, Germany) were applied to prove functional groups within prepared hydrogels in order to confirm the successful copolymerization [23]. A certain amount of hydrogel samples and KBr were evenly mixed at the weight ratio of 1:100 to identify the trend of functional groups more accurately and then pressed to a tablet. The sample tablets were then placed in the FT-IR spectrometer for testing. The spectrum range was 4000–400 cm^{-1}.

The microstructure of the hydrogels played the important role because the water absorbency of hydrogels depends on their porosity [24]. Scanning electron microscopy (SEM, HITACHI-SU8010, Japan) was used to examine the structural morphology of the PNIPAM/γ-PGA/PEG hydrogels (after equilibrium swelling). To preserve the original structural porosity, the hydrogels of equilibrium swelling were dried in a freeze dryer.

Differential scanning calorimetry (DSC, TA Q2000, US) was used to

Table 1
Different dosages of the compositions of PNIPAM/γ-PGA/PEG hydrogels.

Factors	Ratios	Dosages (g)				
		NIPAM	γ-PGA	PEG	Initiator	Cross-linker
NIPAM:γ-PGA	20:1	1.0000	0.0500	0.7500	0.0050	0.0050
	20:2	1.0000	0.1000	0.7500	0.0050	0.0050
	20:3	1.0000	0.1500	0.7500	0.0050	0.0050
	20:4	1.0000	0.2000	0.7500	0.0050	0.0050
NIPAM:PEG	4:1	1.0000	0.2000	0.2500	0.0050	0.0050
	4:2	1.0000	0.2000	0.5000	0.0050	0.0050
	4:3	1.0000	0.2000	0.7500	0.0050	0.0050
	4:4	1.0000	0.2000	1.0000	0.0050	0.0050
Initiator:NIPAM	0.35:100	1.0000	0.2000	1.0000	0.0035	0.0050
	0.50:100	1.0000	0.2000	1.0000	0.0050	0.0050
	1.00:100	1.0000	0.2000	1.0000	0.0100	0.0050
	1.50:100	1.0000	0.2000	1.0000	0.0150	0.0050
Cross-linker:NIPAM	0.35:100	1.0000	0.2000	1.0000	0.0100	0.0035
	0.50:100	1.0000	0.2000	1.0000	0.0100	0.0050
	1.00:100	1.0000	0.2000	1.0000	0.0100	0.0100
	1.50:100	1.0000	0.2000	1.0000	0.0100	0.0150

measure the hydrogel LCST [25]. The measurement was carried out in a nitrogen atmosphere (20 mL/min) at a heating rate of 5 °C/min from 0 to 80 °C.

ESR, which was an important parameter reflecting the water absorption ability of the hydrogels, was estimated using the gravimetric method here. In detail, dry hydrogel (0.2 g) was placed in dialysis bag and immersed in DI water (150 mL) for 80 h until no more hydrogel swelling was observed, and taken out it. Before being weighed, the hydrogel was gently wiped with filters to eliminate moisture errors on the hydrogel surface. The ESR of hydrogels was calculated by the formula (1) below [14]:

$$ESR = \frac{W_s - W_d}{W_d} \quad (1)$$

where W_d is the weight (g) of the pre-weighed dry hydrogel before test; and W_s is the weight (g) of the hydrogel in equilibrium swelling after soaking.

In the dewatering process, the swollen hydrogel was placed in water-bath (40 °C) for dewatering, and its weight alteration was recorded at 5-minute intervals. Eq. (2) was used to calculate the water recovery rate (R) [26]:

$$R = \frac{W_1}{W_0} \times 100\% \quad (2)$$

where W_1 represents the weight (g) of the water released during the thermal stimuli dewatering test; and W_0 represents the weight (g) of water contained in the swollen hydrogel before the dewatering test.

2.4. Optimization of the PNIPAM/γ-PGA/PEG hydrogel preparation conditions by RSM

The Box-Behnken design (BBD) model was used to statistically optimize the parameters with the ESR of PNIPAM/γ-PGA/PEG hydrogel as the response [27]. Although the hydrogel ESR and dewatering ratio increased with the PEG addition, semi-fluid of the hydrogel was prepared when PEG was over dosed (PNIPAM:PEG = 1:2). So, it was meaningless that PEG was optimized by RSM. The initiator (X_1), cross-linker (X_2) and γ-PGA (X_3) were selected as the independent variables for the optimization of the PNIPAM/γ-PGA/PEG hydrogel. In this model, the relations between the coded values and the real values were compared using Eq. (3) [28]:

$$x_i = (X_i - X_0)/\Delta X_i \quad (3)$$

where x_i is the encoded value of the variable (-1, 0, $+1$), X_i is the truth value of the independent variables, X_0 is the truth value of an independent variable at the centre point, and ΔX_i is the step change value.

As shown in Table 2, each variable had three levels in this model. Therefore, 17 experiments, including 5 repeat operations of the central point, were performed to estimate the pure error sum of squares. The ranges of the levels of the independent variables and the design experiments were shown in Table 3. Eq. (4) was used to predict the response values [29]:

$$Y = \beta_0 + \sum \beta_i x_i + \sum \beta_{ii} x_i^2 + \sum \beta_{ij} x_i x_j + \varepsilon \quad (4)$$

where Y represents the predictions; β_0, β_i, β_{ii} and β_{ij} represent the constant regressive coefficients in model; x_i and x_j represent the independent variables in the shape of encoded values; and ε represents the stochastic error ($i = 1 \rightarrow 3$; $j = 1 \rightarrow 3$; $i \neq j$).

Table 2
Actual and coding values of the independent variable parameters.

Independent variable X	Levels		
	−1	0	1
X_1: Initiator (%)	0.50	1.00	1.50
X_2: Cross linker (%)	0.50	1.00	1.50
X_3: γ-PGA (g)	0.10	0.15	0.20

Table 3
The results of three experimental variables in coded units designed by RSM.

Run	Independent variable						Water absorption capacity (g/g)	
	X_1		X_2		X_3		Predicted	Actual
1	0	1.00	−1	0.50	1	0.20	91.50	97.43
2	1	1.50	1	1.50	0	0.15	57.20	56.80
3	−1	0.50	−1	0.50	0	0.15	98.56	99.01
4	−1	0.50	0	1.00	1	0.20	69.05	62.25
5	1	1.50	0	1.00	−1	0.10	62.25	63.40
6	0	1.00	−1	0.50	0	0.15	67.00	62.25
7	0	1.00	0	1.00	0	0.15	67.25	61.09
8	0	1.00	0	1.00	0	0.15	67.25	75.01
9	0	1.00	1	1.50	−1	0.10	55.15	50.35
10	0	1.00	−1	0.50	−1	0.10	87.12	82.50
11	0	1.00	0	1.00	0	0.15	67.25	62.25
12	1	1.50	0	1.00	1	0.20	88.48	87.15
13	0	1.00	0	1.00	0	0.15	67.25	66.70
14	−1	0.50	1	1.50	0	0.15	72.04	75.50
15	0	1.00	1	1.50	1	0.20	55.15	61.20
16	−1	0.50	0	1.00	−1	0.10	60.05	66.25
17	0	1.00	0	1.00	0	0.15	67.25	67.40

Following the test design in Table 3, the aim of the experiment was to measure the response values. The experimental data were processed and analysed through the Design-Expert.8.0.6 software (STAT-EASE Inc., Minneapolis, USA).

The data collected in this work were statistically analysed by the analysis of variance (ANOVA) test. The $p < 0.05$ denoted the differences possessing statistical significance. The F and p value were executed by the Design-Expert software to judge the effectiveness of BBD model. Based on the RSM results, the optimum preparation condition of the hydrogel was determined.

2.5. FO performance evaluation of the optimum hydrogel

The FO performance of the PNIPAM/γ-PGA/PEG hydrogels was studied by using a homemade FO setup (Fig. 1). In the FO experiments, the hydrogels (0.2000 g) were placed on one side of the FO membrane with an active surface area of 3.00 cm^2. The other side of the membrane was exposed to DI water or NaCl solutions with different concentrations. The weight of the hydrogel increased as the pure water permeates through membrane from the feed solution into the draw agent. The FO water flux (F) was calculated according to Eq. (5) [30]:

$$F = \frac{V}{A \times t} \quad (5)$$

where V represents the volume (L) of the water permeating through the membrane to the side of draw agent, which was based on the mass addition of the swelling hydrogel measured over a certain time period; A represents the valid membrane area (m^2); and t represents the performing time (h) of the FO process.

To confirm the reusability of the PNIPAM/γ-PGA/PEG hydrogel, the swelling hydrogel after the FO process was dewatered in a 40 °C water-bath for 30 min [31]. After 0.5 h, the regenerated hydrogel was reused in FO test. Three of this cycle was required to carry out.

To evaluate the properties of PNIPAM/γ-PGA/PEG hydrogel comparably, PNIPAM/γ-PGA hydrogel was prepared via above polymerization process. The ratio of reactant dosage was NIPAM (1.0000 g):γ-PGA = 5:1 and initiator:cross linker:NIPAM = 1:1:100, which was consistent with the optimized PNIPAM/γ-PGA/PEG hydrogel by RSM. Then, the characterization analysis and FO performance evaluation of PNIPAM/γ-PGA hydrogel was performed to compared with PNIPAM/γ-PGA/PEG hydrogel.

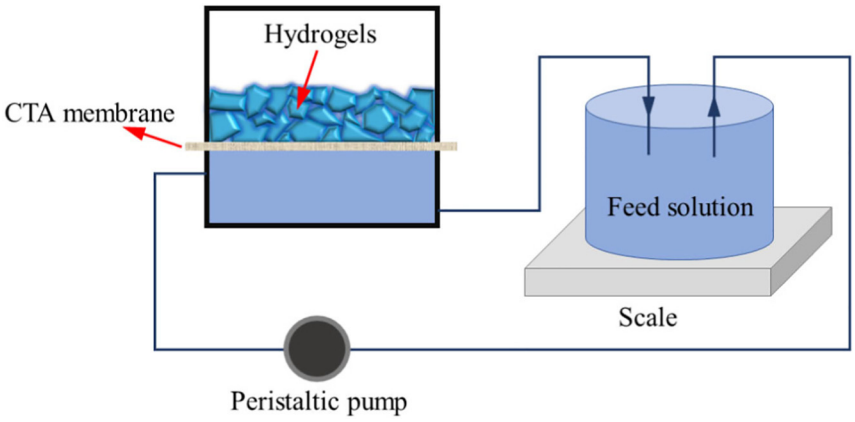

Fig. 1. Schematic diagram of the FO setup.

3. Results and discussion

3.1. Effect of single factor on the hydrogels swelling and dewatering properties

To investigate the effect of reactants of hydrogel on the water absorption, PNIPAM/γ-PGA/PEG hydrogels with different proportions of various additives were examined in the swelling test. Fig. 2 showed the ESR of the hydrogels as a function time.

It was reported that the swelling of hydrogel was driven by the osmotic pressure originating from the interaction between ionic and hydrophilic groups and water molecular [32]. As an ionic polymer, γ-PGA had both ionic group (-COOH) and hydrophilic groups (-NH and -COOH) [20,33]. Therefore, it was proved that the introduction of γ-PGA enhanced the water absorption capacity of PNIPAM/γ-PGA/PEG hydrogels. As shown in Fig. 2A, an increase of the γ-PGA from 5% to 20% enhanced the ESR from 34.98 to 71.14 g/g. Improving of the dosage of PEG increased the ESR as well, which was supported by the results in Fig. 2B. ESR was added up to 58.41 g/g when the NIPAM:PEG ratio was 4:4. The results would be explainable by various porous structures that PEG created in PNIPAM/γ-PGA/PEG hydrogels. It has reported that with the increase of PEG content, the pore structure of hydrogel was more obvious [34,35]. During water absorption, adequate diffusion paths and storage space were provided to enhance ESR of hydrogel. In the actual experiments, fifth weight proportions of NIPAM and PEG = 1:2 was designed. However, semi-fluid state of this

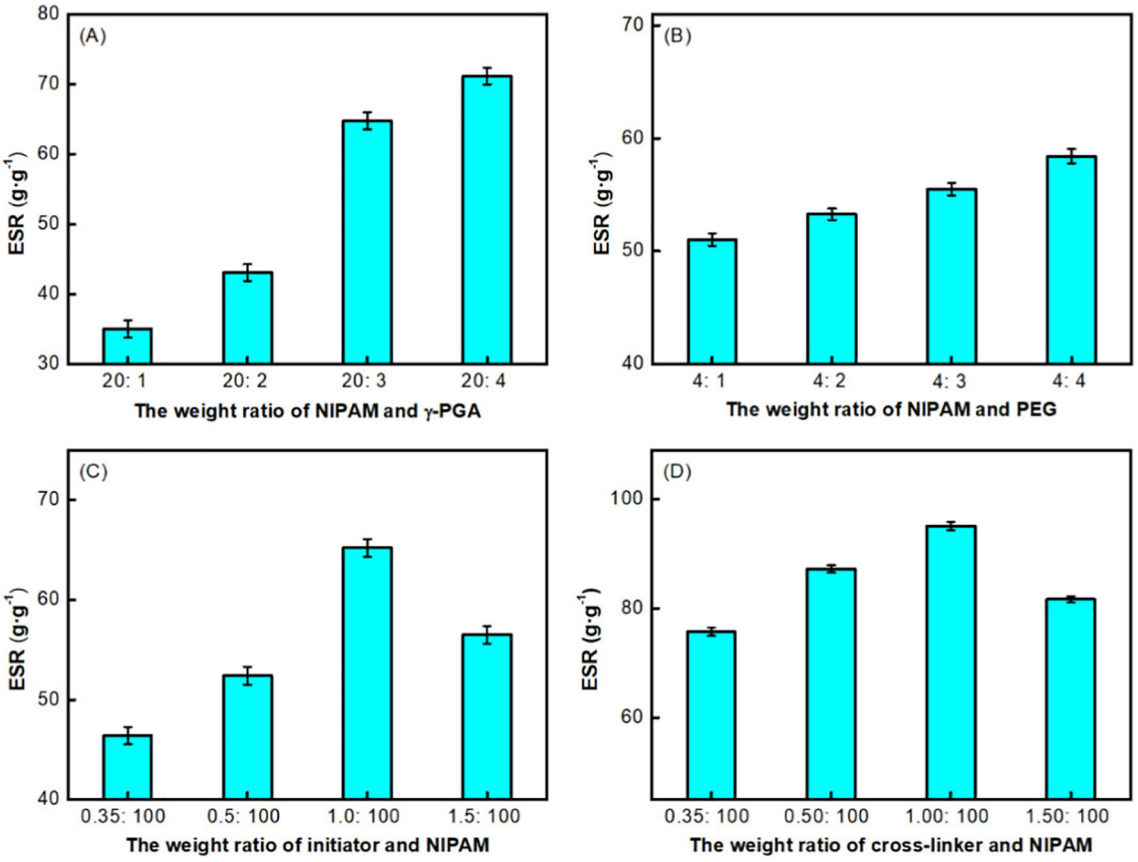

Fig. 2. Effects of different preparation parameters on the ESR of PNIPAM/γ-PGA/PEG hydrogels: the weight ratios of NIPAM and γ-PGA (A); the weight ratios of NIPAM and PEG (B); the weight ratios of initiator and NIPAM (C); and the weight ratios of cross-linker and NIPAM (D).

prepared hydrogel made it unsuitable for application in this FO process.

Combined with the result in Fig. 2A and B, the contribution of γ-PGA seemed to be higher than that of neutral PEG for ESR. An increase in γ-PGA content from 5% to 20% increased the ESR by about 103% whereas an increase in PEG content from 20% to 50% increased the ESR only by 14%. It has been recognized that a neutral hydrogel composed of PEG swelled up to about 50 g/g water content, whereas a charged hydrogel composed of poly (acrylic acid) (PAA) or a similar polyacid swelled up to 90 g/g water content [20,36].

Fig. 2C showed the influence of the weight ratios of the initiator and NIPAM on ESR of PNIPAM/γ-PGA/PEG hydrogels. Better ESR (65.20 g/g) was obtained at the intermediate proportion of initiator:NIPAM = 1.00:100. At a small proportion (initiator:NIPAM = 0.35:100), the number of active radicals created by initiator was not sufficient to form hydrogels with appropriate structure, resulting in a poor ESR of the hydrogel. The same result was seen at initiator:NIPAM = 1.50:100. The addition of excessive initiator caused excess active free radicals during polymerization, which initiated undue cross-linking between the polymer chains [31]. As a result, the network structure of the hydrogel was too dense to expand.

Fig. 2D showed the effects of the ratios of the cross-linker and NIPAM on ESR, and it was observed that the influence of the cross-linker on ESR was similar to that of the initiator. Cross-linker was used to link polymer chains to form hydrogels [18]. The highest ESR was 94.76 g/g in the middle proportion (cross-linker:NIPAM = 1.00:100). For a low addition of the cross-linker (cross-linker:NIPAM = 0.35:100), the polymer chains cannot be sufficiently cross-linked and the structure of failed to form completely, resulting in a low ESR. When superfluous cross-linker (cross-linker:NIPAM = 1.50:100) was added, excessive cross-linking of polymer chains resulted in an overly dense hydrogel structure, increasing the difficulty in water transmission in hydrogel. The influences of the initiator and cross-linker in terms of hydrogels structure and ESR were consistent with existing literature [37]. Overall, these results were favourable for conducting RSM experiments to further explore the interaction among the reactants (PNIPAM, γ-PGA, PEG, initiator and cross-linker).

Due to the thermo-sensitive phase transition behaviours of the hydrogels, the hydrogel chains changed from hydrophilic state to hydrophobic state and gradually shrank to release water above their LCST [38]. Refer to previous literatures, the dewatering was performed in water bath at 40 °C for 30 min [4]. An interesting phenomenon was that all PNIPAM/γ-PGA/PEG hydrogels could achieve dewatering equilibrium only required temperature variation of 15 °C (from room temperature to 40 °C). It was showed in Fig. 3.

Fig. 3A showed the effects of varying γ-PGA concentrations (NIPAM:γ-PGA ratio from 20:1 to 20:4) on the water recovery rates of the PNIPAM/γ-PGA/PEG hydrogel. With increasing the dosage of γ-PGA, the water recovery rate decreased and the time to reach the deswelling equilibrium was prolonged. For example, the hydrogel (NIPAM:γ-PGA = 20:1) reached dewatering equilibrium (97.4%) at 5 min while the hydrogel (NIPAM:γ-PGA = 20:4) yielded 88% water consuming 30 min. At high γ-PGA concentration, most of free water in hydrogel existed in the form of bound water combined with ionic and hydrophilic groups of γ-PGA, which weaken the temperature response of the hydrogels and increase the difficulty of dewatering [39,40]. Therefore, more energy or heat was required to break these bonds, leading to the prolongation of dewatering and the reduction of water recovery rate [41,42]. Moreover, the influence of dosages of PEG on the water recovery rate of the PNIPAM/γ-PGA/PEG hydrogel was shown in Fig. 3B. Improving the amount of PEG increased the water recovery rate and shortened the time to reach dewatering equilibrium. Representatively, the water recovery rate for NIPAM:PEG = 4:4 was 97.31% at t = 10 min, which was higher than 90.04% for NIPAM:PEG = 4:1 at t = 30 min. For non-porous hydrogel, a common problem was that in the early stage of dewatering, a dense layer on the hydrogel surface hindered the water diffusion and release from the hydrogel [43,44]. But in fact, the results in Fig. 3B could be illustrated that this issue was clearly compromised through the introduction of porous structure in hydrogel. The porous structure generated by PEG enhanced the capillary driving force of hydrogel and provided more channels for water release [45]. Therefore, the PNIPAM/γ-PGA/PEG hydrogels could achieve rapid dewatering at high water recovery rate.

The effects of initiator concentrations on the water recovery rate were shown in Fig. 3C. Higher water recovery rate of 95.15% was achieved at initiator:NIPAM = 1.00:100 only 10 min. But the weaker water recovery rates of 90.37% (for initiator:NIPAM = 0.35:100) and 94.38% (for initiator:NIPAM = 1.50:100) at 30 min. The dosage of initiator directly affected the chemical structure of hydrogel in polymerization process so that the hydrogels showed different dewatering properties [46,47]. When initiator concentration was low (initiator:NIPAM = 0.35:100 and initiator:NIPAM = 0.50:100), the slow polymerization process resulted in loose space volume in hydrogel structure. For superfluous initiator content (initiator:NIPAM = 1.50:100), the hydrogel would have smaller space size at fast polymerization rate [48,49]. In short, too loose or too dense structure of hydrogel was not conductive to release water during dewatering. Fig. 3D showed the effects of the cross-linker content on the water recovery rates. Although the tendency of the hydrogels flattened out to reach dewatering equilibrium compared with hydrogel in Fig. 3C, the highest water recovery rate of 97.64% was achieved at cross-linker:NIPAM = 1.00:100 at t = 20 min. Thus, the water retained in the PNIPAM/γ-PGA/PEG hydrogels could be efficiently recovered. The structure of the hydrogel was gradually strengthened with increasing cross-linker, leading to the continuous enhance in water recovery rate. However, excessive amount of the cross-linker (cross-linker:NIPAM = 1.50:100) reduced the water recovery rate due to the too dense structure of hydrogel hindered the removal of water molecules [50,51]. It was worth mentioning that water recovery rates of all hydrogels were higher than 87.99%, which exhibit excellent dewatering property at low temperature (40 °C).

3.2. PNIPAM/γ-PGA/PEG hydrogel optimization by RSM

The ANOVA data of BBD examined the statistical significance of the model terms (Table 4). Values of "prob. > *F*" less than 0.0500 indicated that the model terms were significant. In the circumstances, X_2 and X_1X_3 were significant model terms ($p < 0.0500$) and performed critical roles in tuning the ESR of PNIPAM/γ-PGA/PEG hydrogels. The Lack of Fit "*F*-value" was 3.45 (> 0.0500), which indicated that the Lack of Fit was not significant. These results indicated the adequacy of the BBD model, which could guide the design of PNIPAM/γ-PGA/PEG hydrogels with high ESR [52].

BBD model was examined through various diagnostic plots (Fig. 4) to further prove that the results of the fitted response model were more accurate [29]. There were 17 points in Fig. 4A, corresponding to the 17 sets of water absorption capacity data (predicted and actual) in Table 3. The predicted and actual values presented linear correlation, which were closely spaced along the diagonal line. As shown in Fig. 4B, all data between −2 and 2 were above 95% confidence level. The residual normal distribution was used to further investigate the reliability of the experimental results, as shown in Fig. 4C. In conclusion, these data obtained from RSM could be used to optimize the preparation parameters of the hydrogels. 3D surface maps representing the combination of the factors in scheme design were shown in Fig. 5. The result was draw that the ESR was significantly dependent on cross-linker and the interaction between initiator and γ-PGA. While the PNIPAM/γ-PGA/PEG hydrogels have indeed demonstrated enhanced osmotic pressure, the addition of excessive γ-PGA hindered their temperature response. Therefore, there was an inherent trade-off between the high osmotic pressure and excellent dewatering performance when it came to the choice of γ-PGA concentration. Combined with single factor experiment and RSM, the optimal preparation scheme of PNIPAM/γ-PGA/PEG

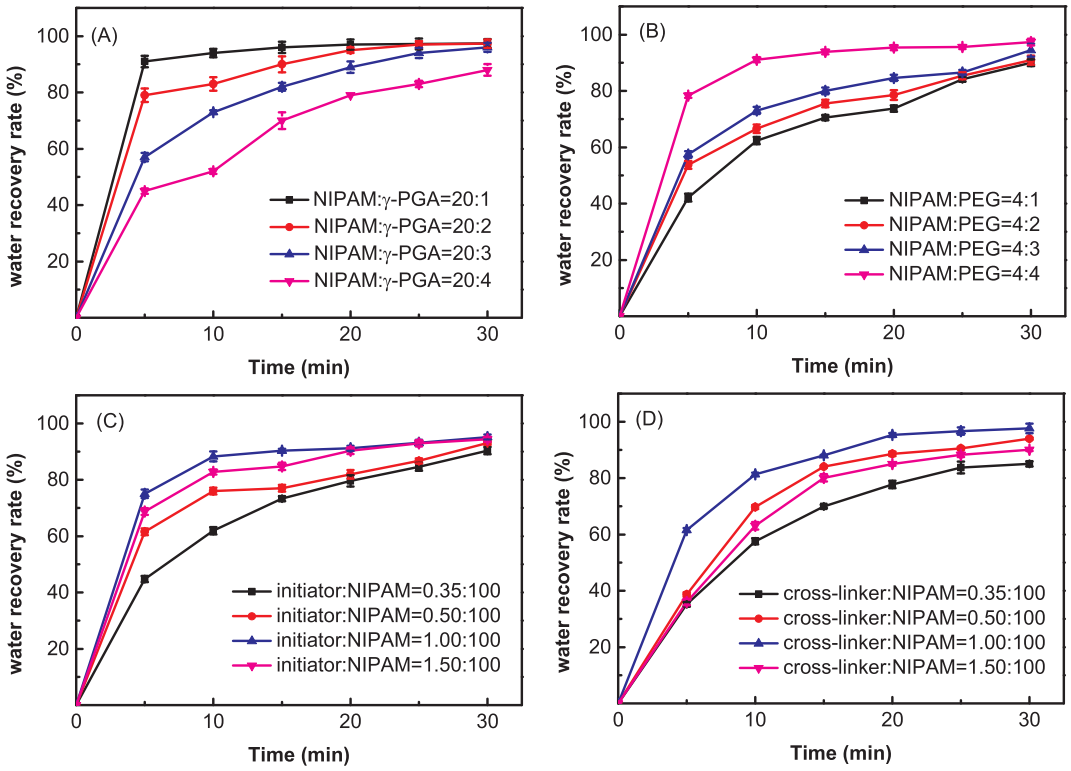

Fig. 3. Effects of different preparation parameters on the water recovery rate of the PNIPAM/γ-PGA/PEG hydrogels: the weight ratios of NIPAM and γ-PGA (A); the weight ratios of NIPAM and PEG (B); the weight ratios of initiator and NIPAM (C); and the weight ratios of cross-linker and NIPAM (D).

hydrogel was determined as NIPAM:γ-PGA:PEG = 5:1:5 and initiator:cross-linker:NIPAM = 1:1:100.

3.3. Structure and properties of the PNIPAM/γ-PGA/PEG hydrogels

The FT-IR spectra of PNIPAM/γ-PGA and PNIPAM/γ-PGA/PEG hydrogel were similar in Fig. 6. NIPAM displayed characteristic peaks at 3455 and 2918 cm^{-1}, corresponding to the N—H and CH_2 stretching, respectively. The characteristic peaks at 1651 and 1564 cm^{-1} were due to the C═O stretching and N—H bending, respectively. The characteristic peaks at 1300 and 2979 cm^{-1} were attributed to the C-N-H and C—H symmetric stretching. The existence of the characteristic peak at 2979 cm^{-1} indicated the presence of γ-PGA in both PNIPAM/γ-PGA and PNIPAM/γ-PGA/PEG hydrogel [50]. For PNIPAM/γ-PGA/PEG hydrogel, there was no obvious peak appearing around 1100 cm^{-1} of PEG in the spectra after PEG addition. It was recognized that PEG was embedded in the hydrogel structure rather than participated in the polymerization reaction. After that it was removed in the washing process [53]. In addition, it was also found that the molecular structure of PNIPAM/γ-PGA/PEG hydrogel was not affected by PEG addition due to the original functional groups were knowable.

Fig. 7A and B showed the surface morphology of PNIPAM/γ-PGA and PNIPAM/γ-PGA/PEG hydrogel respectively. Compared with the nonporous compact of PNIPAM/γ-PGA hydrogel, PNIPAM/γ-PGA/PEG hydrogel successfully developed obvious porous structure due to PEG addition. This result was consistent with the literatures reported [54]. They were super-porous structures with pore sizes in the range of 1.26–24.92 μm (see more SEM details in Fig. S1). Most of spherical super-pores inside hydrogel were connected to form open channels system, which acts a capillary system causing rapid water uptake and dewatering [55]. Combined with the undetected PEG peaks in FT-IR (Fig. 6), it was proved again that PEG was only embedded in hydrogel and did not react with other monomers during the polymerization [56]. The hydrogels were favourably produced with super-porous structure

Table 4
ANOVA for response parameters.

Source	Sum of squares	d.f.	Mean square	F value	*p*-Value prob. > F	Significant/non-significant
BBD model	2683.39	9	298.15	6.85	0.0095	Significant
X_1-initiator	110.62	1	110.62	2.54	0.1550	
X_2-cross-linker	2266.90	1	2266.90	52.05	0.0002	Significant
X_3-γ-PGA	8.53	1	8.53	0.20	0.6715	
X_1X_2	8.02	1	8.02	0.18	0.6807	
X_1X_3	18.91	1	18.91	0.43	0.0410	Significant
X_2X_3	4.01	1	4.01	0.092	0.7704	
X_1^2	14.75	1	14.75	0.34	0.5789	
X_2^2	233.39	1	233.39	5.36	0.0538	
X_3^2	19.62	1	19.62	0.45	0.5237	
Residual	304.87	7	43.55			
Lack of fit	219.83	3	73.28	3.45	0.1315	
Pure error	85.04	4	21.26			
Sum	2988.26	16				

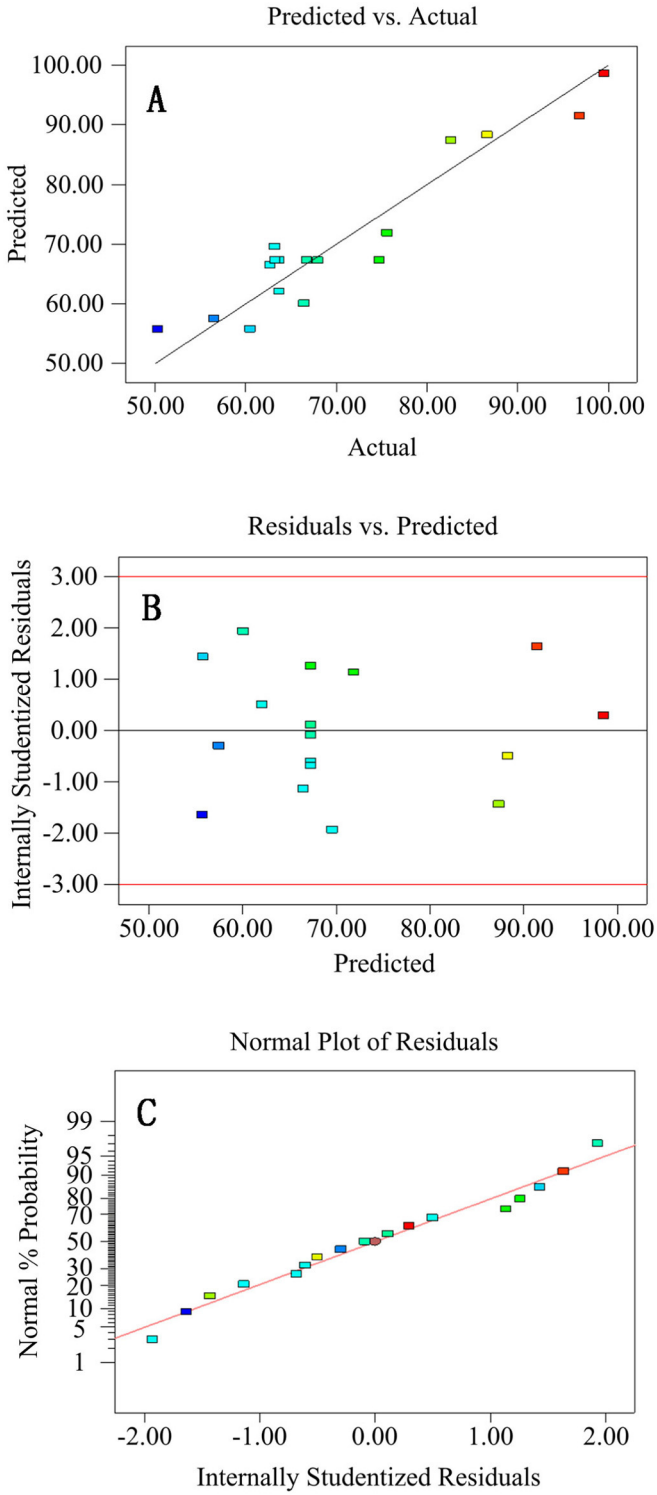

Fig. 4. Analysis of the response surface: plot of Predicted versus Actual (A); plot of Residuals versus Predicted (B); and Normal Plot of Residuals (C).

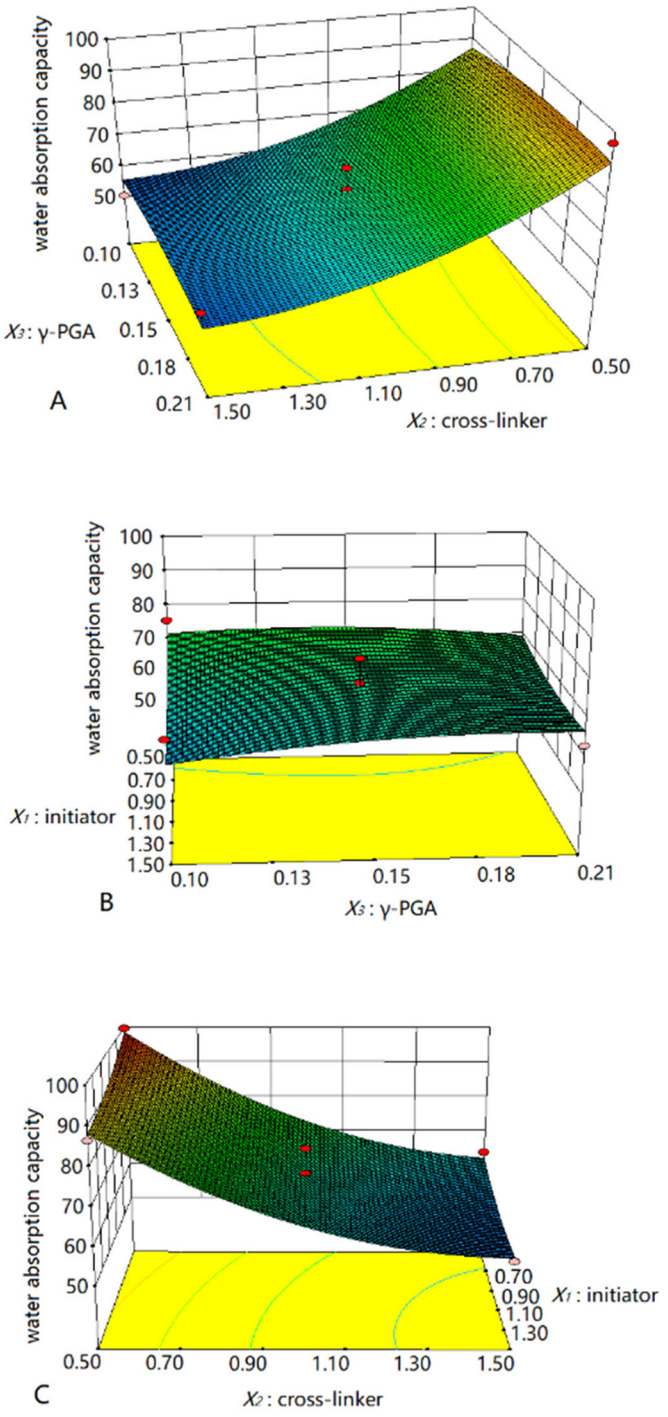

Fig. 5. Response surface images: the cross-linker and γ-PGA (A); initiator and γ-PGA (B); and initiator and cross-linker (C).

after PEG washed away.

The LCST of PNIPAM/γ-PGA and PNIPAM/γ-PGA/PEG hydrogels were determined by the DSC curves measurement in Fig. 8. The LCSTs of 35.54 °C and 35.20 °C were represented in obvious endothermic peaks located on PNIPAM/γ-PGA and PNIPAM/γ-PGA/PEG hydrogel curves, respectively. As previously reported, PNIPAM hydrogel exhibited the superior LCST of 32 °C [57].Compared with PNIPAM hydrogel, the LCST of PNIPAM/γ-PGA hydrogel slightly increased due to the presentation of ionic groups of γ-PGA increased the heat or energy demand for hydrogel dewatering [7,33]. The phase transition temperature of PNIPAM/γ-PGA/PEG hydrogel was reduced by the superporous structure generated by PEG [56]. Therefore, PNIPAM/γ-PGA/PEG hydrogel exhibited excellent thermal sensitivity, which could achieve efficient regeneration for the reduction of energy consumption in FO process.

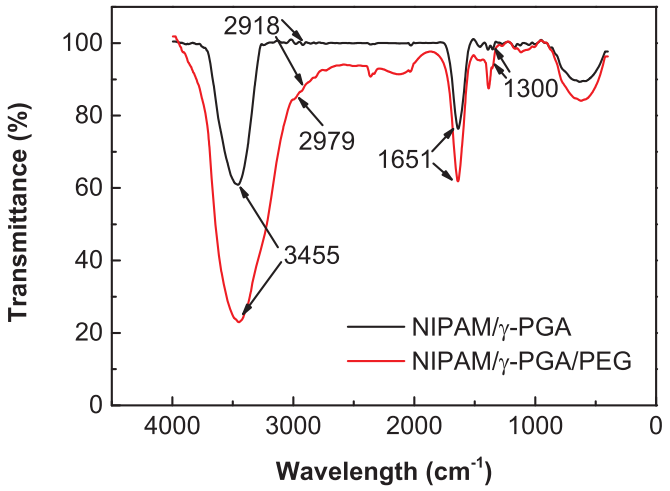

Fig. 6. FT-IR spectra of the PNIPAM/γ-PGA (NIPAM:γ-PGA = 5:1, initiator:cross linker:NIPAM = 1:1:100) and PNIPAM/γ-PGA/PEG hydrogel (NIPAM:γ-PGA:PEG = 5:1:5, initiator:cross-linker:NIPAM = 1:1:100).

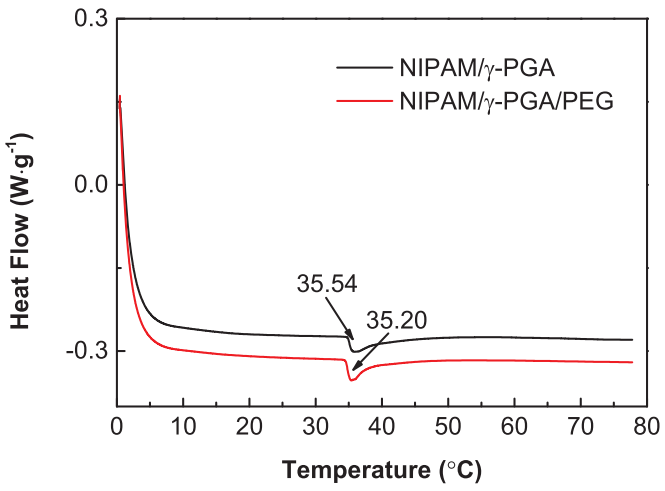

Fig. 8. DSC results: PNIPAM/γ-PGA (NIPAM:γ-PGA = 5:1; initiator:cross linker:NIPAM = 1:1:100); and PNIPAM/γ-PGA/PEG hydrogel (NIPAM:γ-PGA:PEG = 5:1:5; initiator:cross-linker:NIPAM = 1:1:100).

3.4. Evaluation of the optimum PNIPAM/γ-PGA/PEG hydrogel as the draw agent in FO process

Fig. 9 showed the water fluxes induced by the swelling of PNIPAM/γ-PGA and PNIPAM/γ-PGA/PEG hydrogel as a function of time in 12-h FO process. In the first 0.5 h, the highest water flux was 1.99 LMH generated by PNIPAM/γ-PGA/PEG hydrogel, which was higher than PNIPAM/γ-PGA (1.41 LMH) and pure NIPAM (0.30 LMH at 0.2 wt%) [12]. It is concluded the permeability of PNIPAM/γ-PGA/PEG hydrogel was closely related to the incorporation of ionic γ-PGA and pore-forming PEG. Previously, the water absorption capacity of PNIPAM/γ-PGA/PEG hydrogel has been maximized by tailoring the proportion of reactants in previous experiments of swelling (Fig. 2) and RSM (Fig. 5). As the FO process proceeded (about 2 h), the water fluxes for both hydrogels decreased gradually due to their osmotic pressure decreased with an increasing degree of swelling. This similar tendency has also been reported in the FO process using P (NIPAM-co-SA) hydrogel as draw agent [12].

Fig. 10 presented the water fluxes of PNIPAM/γ-PGA/PEG hydrogel in a 12 h FO process employing NaCl solution with different concentrations as feed solution. With increasing concentration of salt in feed, the initial water flux decreased created by PNIPAM/γ-PGA/PEG

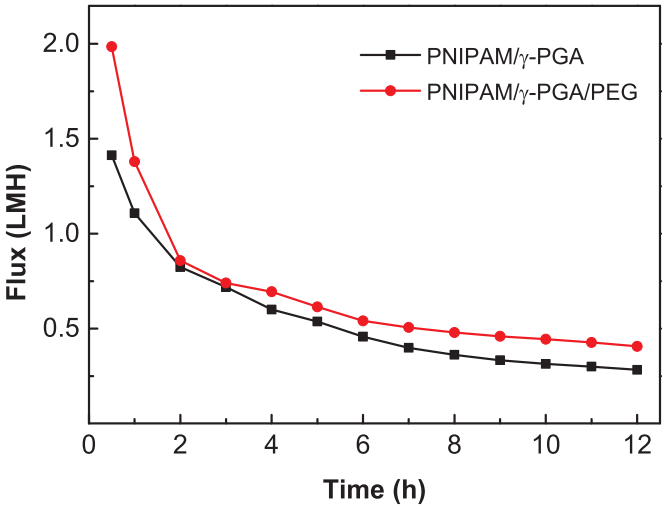

Fig. 9. Water fluxes in the 12 h FO process using PNIPAM/γ-PGA and PNIPAM/γ-PGA/PEG hydrogel as the draw agents.

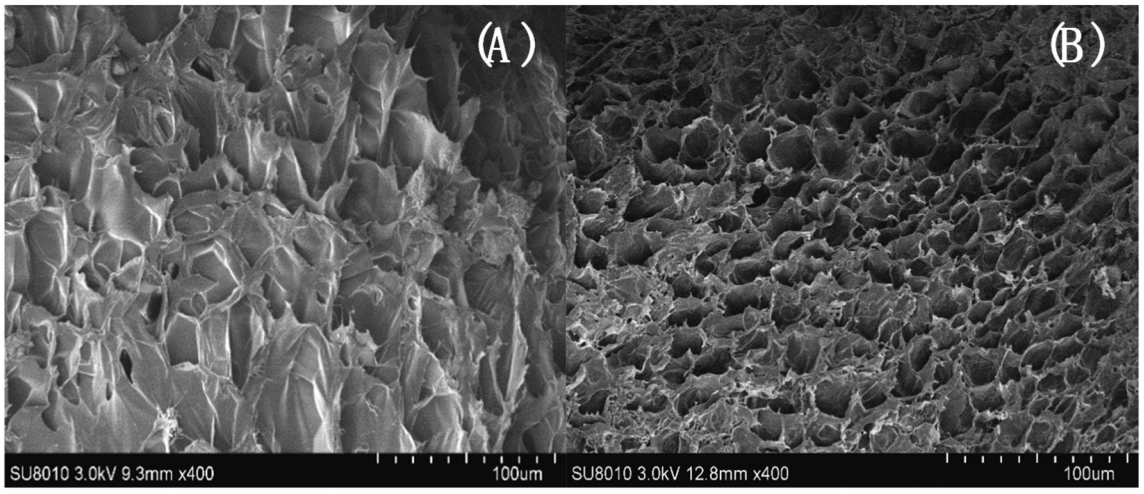

Fig. 7. SEM images:PNIPAM/γ-PGA (NIPAM:γ-PGA = 5:1; initiator:cross linker:NIPAM = 1:1:100) (A); and PNIPAM/γ-PGA/PEG hydrogel (NIPAM:γ-PGA:PEG = 5:1:5; initiator:cross-linker:NIPAM = 1:1:100) (B).

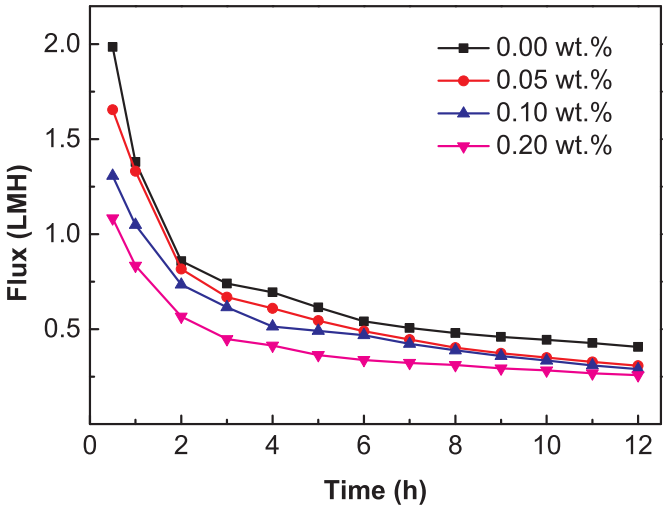

Fig. 10. Water flux in 12 h FO process using the PNIPAM/γ-PGA/PEG hydrogel as the draw agent and NaCl solution with different concentrations as feed solution.

hydrogel draw agent. It could be interpreted that the reduction of osmotic pressure gradient between PNIPAM/γ-PGA/PEG and feed due to the increment of salt concentration in feed solution [44]. Furthermore, the desalination ability of hydrogel was caused by the Donnan-like partitioning of salt ions due to ionic groups of γ-PGA [58]. Meanwhile, more water absorption capacity was provided by porous structure of PNIPAM/γ-PGA/PEG hydrogel in incorporation of PEG. Both of these worked together to enhance the FO water flux and maintain it for an extended long period.

The water flux test was carried out to confirm the reusability of PNIPAM/γ-PGA/PEG hydrogel. Fig. 11 showed the time courses of water fluxes for three cycles of water adsorption to dewatering, employing the DI water as feed. At initial 0.5 h, the water fluxes generated by the recycled hydrogels (recycle 1, recycle 2 and recycle 3) were observed at 1.99, 1.68 and 1.42 LMH, respectively. The flux performance of PNIPAM/γ-PGA/PEG hydrogel reduced after each regeneration. However, they were still superior to that of fresh PNIPAM/γ-PGA hydrogel (1.41 LMH) in Fig. 9. The main reason for the high flux may be that the swelling pressure of reused hydrogel could be completely recovered during dewatering (almost 100%) [59]. The PNIPAM/γ-PGA/PEG hydrogel could maintain high water flux and efficient water

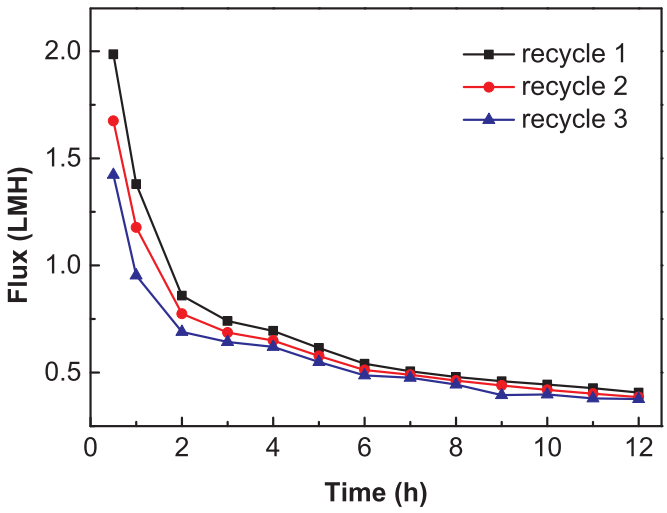

Fig. 11. Water flux as a function of 12 h time produced by the recycled PNIPAM/γ-PGA/PEG hydrogels as draw agent.

recovery ability, which was confirmed by the water recovery test (in Fig. 3) and the cycles of water flux (Fig. 11).

Table 5 showed the comparison of FO flux and regeneration performance of NIPAM/γ-PGA/PEG hydrogel with that of other ionic draw agents with temperature response. Although the FO flux of NIPAM/γ-PGA/PEG hydrogel (1.08 LMH) was comparable to data reported for PSA, PSA did not exhibit phase transition by changing temperature [60]. The FO flux of NIPAM/γ-PGA/PEG hydrogel was better than other draw agents composited with ionic polymer, e.g., PNIPAM-SA-C (~0.77 LMH) [10] and PNIPAM-IPN-PVA (~0.23–0.24 LMH) [8]. It was particularly noteworthy that the regeneration of NIPAM/γ-PGA/PEG hydrogel at lower LCST (35.20 °C) was more efficient than the other hydrogels. The NIPAM/γ-PGA/PEG hydrogel exhibited the significant advantage of almost 100% water recovery rate, which could be easier to regenerate than other ionic hydrogels such PSA and PAA [61,62]. In this work, NIPAM offered the excellent thermal responsive for the developed hydrogel, γ-PGA endowed the high osmotic pressure for it as well, and PEG provided super-porous structure for water release. Hence, ionic thermo-responsive NIPAM/γ-PGA/PEG hydrogel was a superior candidate for improving FO process.

4. Conclusion

In this work, the ionic thermo-responsive hydrogels composed of NIPAM, γ-PGA and PEG were successfully synthesized via polymerization. The enhanced ESR of the PNIPAM/γ-PGA/PEG hydrogels was proved to be significantly dependent on the incorporation of ionic γ-PGA. PEG was mainly used to optimize the pore structure of hydrogel to create more water paths, which was conductive to the efficient dewatering of hydrogel. The optimal preparation scheme of hydrogel was obtained: NIPAM:γ-PGA:PEG = 5:1:5 and initiator:cross-linker:NIPAM = 1:1:100 by single factor test and RSM. It was also demonstrated that the water fluxes of the optimal PNIPAM/γ-PGA/PEG hydrogel had significant enhancement. Employing DI water, 0.05, 0.1 and 0.2 wt% NaCl solution as the feed, the initial water fluxes of PNIPAM/γ-PGA/PEG hydrogel were 1.99, 1.65, 1.31 and 1.08 LMH within 0.5 h, respectively. In addition, the optimal PNIPAM/γ-PGA/PEG hydrogel showed promising recyclability, which of water fluxes were 1.99, 1.68 and 1.42 LMH within 0.5 h for three cycles. This work warrants further studies and development focusing on the practical application of PNIPAM/γ-PGA/PEG hydrogels to desalination in FO process at low cost.

CRediT authorship contribution statement

Keyuan Zhang: Data curation, Investigation, Writing-original draft, Writing - review & Editing. Fei Li: Formal analysis, Software. Yan Wu: Methodology, Investigation. Li Feng: Supervision. Liqiu Zhang: Writing - review & editing.

Declaration of competing interest

The authors declare that they no known competing financial interests or personal relationships that could have appeared to influence the work reported in this paper.

Acknowledgments

We gratefully acknowledge funding from the Fundamental Research Funds for the Central Universities (No. 2015ZCQ-HJ-02), the National Natural Science Foundation of China (41977317), Beijing Natural Science Foundation (No. 8182037), Major Science and Technology Program for Water Pollution Control and Treatment (No. 2018ZX0731007) and Shenzhen Techand Ecology & Environment Co., LTD (THRD009).

Table 5
Comparison of FO flux and regeneration performance with other temperature-responsive hydrogels reported in the literatures.

Hydrogel	FO flux (LMH)	LCST (°C)	Regeneration performance	Reference
PSA	~1.12	No LCST	No experiment	[10]
PNIPAM-SA-C	0.77	No experiments	1.0 kWm^{-2} solar irradiation 1 h 47 °C	[8]
PNIPAM-IPN-PVA	~0.23–0.24	34.12	At 40 °C immersion	[44]
PNIPAM	0.3	32	At 50 °C in the thermal mechanical dewatering cell	[12]
PNIPAM/γ-PGA/PEG	1.08	35.20	Heat in water-bath at 40 °C	This work

Note: 0.20 wt% NaCl solution was employed as feed solution in FO.

Appendix A. Supplementary data

Supplementary data to this article can be found online at https://doi.org/10.1016/j.desal.2020.114667.

References

[1] W.J. Lee, Z.C. Ng, S.K. Hubadillah, P.S. Goh, W.J. Lau, M.H.D. Othman, A.F. Ismail, N. Hilal, Fouling mitigation in forward osmosis and membrane distillation for desalination, Desalination 480 (2020).

[2] W. Suwaileh, N. Pathak, H. Shon, N. Hilal, Forward osmosis membranes and processes: a comprehensive review of research trends and future outlook, Desalination 485 (2020).

[3] N. Akther, A. Sodiq, A. Giwa, S. Daer, H.A. Arafat, S.W. Hasan, Recent advancements in forward osmosis desalination: a review, Chem. Eng. J. 281 (2015) 502–522.

[4] Y. Cai, X.M. Hu, A critical review on draw solutes development for forward osmosis, Desalination 391 (2016) 16–29.

[5] A. Al-Karaghouli, L.L. Kazmerski, Energy consumption and water production cost of conventional and renewable-energy-powered desalination processes, Renew. Sust. Energ. Rev. 24 (2013) 343–356.

[6] S. Al-Obaidani, E. Curcio, F. Macedonio, G.D. Profio, H. Al-Hinai, E. Drioli, Potential of membrane distillation in seawater desalination: thermal efficiency, sensitivity study and cost estimation, J. Membr. Sci. 323 (2008) 85–98.

[7] Y. Hartanto, M. Zargar, H. Wang, B. Jin, S. Dai, Thermoresponsive acidic microgels as functional draw agents for forward osmosis desalination, Environ. Sci. Technol. 50 (2016) 4221–4228.

[8] D. Li, X. Zhang, J. Yao, Y. Zeng, G.P. Simon, H. Wang, Composite polymer hydrogels as draw agents in forward osmosis and solar dewatering, Soft Matter 7 (2011).

[9] Y. Lu, T. Chen, A. Mei, T. Chen, Y. Ding, X. Zhang, J. Xu, Z. Fan, B. Du, Solution behaviors and microstructures of PNIPAm-P123-PNIPAm pentablock terpolymers in dilute and concentrated aqueous solutions, Phys. Chem. Chem. Phys. 15 (2013) 8276–8286.

[10] D. Li, X. Zhang, G.P. Simon, H. Wang, Forward osmosis desalination using polymer hydrogels as a draw agent: influence of draw agent, feed solution and membrane on process performance, Water Res. 47 (2013) 209–215.

[11] R. Ou, H. Zhang, S. Kim, G.P. Simon, H. Hou, H. Wang, Improvement of the swelling properties of ionic hydrogels by the incorporation of hydrophobic, elastic microfibers for forward osmosis applications, Ind. Eng. Chem. Res. 56 (2017) 505–512.

[12] D. Li, X. Zhang, J. Yao, G.P. Simon, H. Wang, Stimuli-responsive polymer hydrogels as a new class of draw agent for forward osmosis desalination, Chem. Commun. (Camb.) 47 (2011) 1710–1712.

[13] D. Zhao, P. Wang, Q. Zhao, N. Chen, X. Lu, Thermoresponsive copolymer-based draw solution for seawater desalination in a combined process of forward osmosis and membrane distillation, Desalination 348 (2014) 26–32.

[14] Y. Hartanto, S. Yun, B. Jin, S. Dai, Functionalized thermo-responsive microgels for high performance forward osmosis desalination, Water Res. 70 (2015) 385–393.

[15] T. Jian, X. Si Zhang, W. Shi Cheng, X. Ren Huang, Zhuo, Temperature-sensitive poly (N-isopropylacrylamide) hydrogels with macroporous structure and fast response rate, Macromolecular Rapid Communications 24 (2003) 447–451.

[16] A. Raic, L. Rodling, H. Kalbacher, C. Leethedieck, Biomimetic macroporous PEG hydrogels as 3D scaffolds for the multiplication of human hematopoietic stem and progenitor cells, Biomaterials 35 (2014) 929–940.

[17] M.F. Akhtar, M. Hanif, N.M. Ranjha, Methods of synthesis of hydrogels … a review, Saudi Pharm. J. 24 (2016) 554–559.

[18] T. Kopac, A. Rucigaj, M. Krajnc, The mutual effect of the crosslinker and biopolymer concentration on the desired hydrogel properties, Int. J. Biol. Macromol. 159 (2020) 557–569.

[19] L. An, A. Wang, J. Chen, Studies on poly(acrylic acid)/attapulgite superabsorbent composite. I. Synthesis and characterization, Journal of Applied Polymer Science 92 (2010) 1596–1603.

[20] S. Chung, C. Gentilini, A. Callanan, M. Hedegaard, S.R. Hassing, M.M. Stevens, Responsive poly (γ-glutamic acid) fibres for biomedical applications, J. Mater. Chem. B 1 (2013) 1397–1401.

[21] N. Broguiere, A. Husch, G. Palazzolo, F. Bradke, S. Madduri, M. Zenobiwong, Macroporous hydrogels derived from aqueous dynamic phase separation, Biomaterials 200 (2019) 56–65.

[22] M. Qasim, N.A. Darwish, S. Sarp, N. Hilal, Water desalination by forward (direct) osmosis phenomenon: a comprehensive review, Desalination 374 (2015) 47–69.

[23] H. Cui, H. Zhang, M. Yu, F. Yang, Performance evaluation of electric-responsive hydrogels as draw agent in forward osmosis desalination, Desalination 426 (2018) 118–126.

[24] Y. Cai, R. Wang, W.B. Krantz, A.G. Fane, X.M. Hu, Exploration of using thermally responsive polyionic liquid hydrogels as draw agents in forward osmosis, RSC Adv. 5 (2015) 97143–97150.

[25] W. Ali, B. Gebert, T. Hennecke, K. Graf, M. Ulbricht, J.S. Gutmann, Design of thermally responsive polymeric hydrogels for brackish water desalination: effect of architecture on swelling, deswelling, and salt rejection, ACS Appl. Mater. Interfaces 7 (2015) 15696–15706.

[26] A. Shakeri, H. Salehi, N. Khankeshipour, M.T. Nakhjiri, F. Ghorbani, Magnetic nanoparticle-crosslinked ferrohydrogel as a novel class of forward osmosis draw agent, Journal of Nanoparticle Research 20 (2018).

[27] M. Moztahida, D.S. Lee, Photocatalytic degradation of methylene blue with P25/graphene/ polyacrylamide hydrogels: optimization using response surface methodology, J. Hazard. Mater. 400 (2020) 1–11.

[28] F.H. Tsai, Y. Kitamura, M. Kokawa, Liquid-core alginate hydrogel beads loaded with functional compounds of radish by-products by reverse spherification: optimization by response surface methodology, Int. J. Biol. Macromol. 96 (2017) 600–610.

[29] L. Zhao, Q. Li, X. Xu, W. Kong, X. Li, Y. Su, Q. Yue, B. Gao, A novel Enteromorpha based hydrogel optimized with Box–Behnken response surface method: synthesis, characterization and swelling behaviors, Chem. Eng. J. 287 (2016) 537–544.

[30] A. Shakeri, H. Salehi, M. Taghvay Nakhjiri, E. Shakeri, N. Khankeshipour, F. Ghorbani, Carboxymethylcellulose-quaternary graphene oxide nanocomposite polymer hydrogel as a biodegradable draw agent for osmotic water treatment process, Cellulose 26 (2018) 1841–1853.

[31] D.J. Johnson, W.A. Suwaileh, A.W. Mohammed, N. Hilal, Osmotic's potential: an overview of draw solutes for forward osmosis, Desalination 434 (2018) 100–120.

[32] J. Zeng, S. Cui, Q. Wang, R. Chen, Multi-layer temperature-responsive hydrogel for forward-osmosis desalination with high permeable flux and fast water release, Desalination 459 (2019) 105–113.

[33] S.J. Park, H. Uyama, M.S. Kwak, M.H. Sung, Comparison of the stability of poly-gamma-glutamate hydrogels prepared by UV and gamma-ray irradiation, J. Microbiol. Biotechnol. 29 (2019) 1078–1082.

[34] S. Romero-Vargas Castrillón, X. Lu, D.L. Shaffer, M. Elimelech, Amine enrichment and poly(ethylene glycol) (PEG) surface modification of thin-film composite forward osmosis membranes for organic fouling control, J. Membr. Sci. 450 (2014) 331–339.

[35] H. Tokuyama, Y. Nakahata, R. Sato, Y. Nagatsu, T. Ban, Mechanical and metal adsorption properties of emulsion gel adsorbents composed of PEGDA-co-PEG hydrogels and tri-n-octylamine, Polym. Bull. 75 (2018) 1597–1606.

[36] S. Kosmella, Advances in polymer science. Vol. 110 responsive gels: volume transitions II edited by K. Dusek, Springer Verlag: Berlin, Heidelberg, New York 1993, X 269 pages, hardcover, DM 198, ISBN 3-540-56970-7, Acta Polym. 45 (2003) 396.

[37] H. Dai, H. Huang, Enhanced swelling and responsive properties of pineapple peel carboxymethyl cellulose-g-poly(acrylic acid-co-acrylamide) superabsorbent hydrogel by the introduction of carclazyte, J. Agric. Food Chem. 65 (2017) 565–574.

[38] S. Kai, L. Zhi, P. Yanxiong, W. Baolong, J. Xiangling, Preparation of macroporous polyvinyl alcohol formaldehyde based hydrogels and their dual thermo- and pH-responsive behavior, Appl. Surf. Sci. 509 (2019) 144754.

[39] S. Murakami, N. Aoki, S. Matsumura, Bio-based biodegradable hydrogels prepared by crosslinking of microbial poly(γ-glutamic acid) with L-lysine in aqueous solution, Polym. J. 43 (2011) 414–420.

[40] S.F. Anis, R. Hashaikeh, N. Hilal, Functional materials in desalination: a review, Desalination 468 (2019).

[41] Ou Ranwen, Huacheng Zhang, Seungju Kim, George P. Simon, Hongjuan, Improvement of the swelling properties of ionic hydrogels by the incorporation of hydrophobic, elastic microfibers for forward osmosis applications, Ind. Eng. Chem. Res 56 (2016) 505–512.

[42] K.L. Tu, G.P. Simon, H. Wang, Fast-responsive monolithic hydrogels as draw agent for forward osmosis membrane process, Sep. Sci. Technol. 52 (2017) 2583–2590.

[43] V. Schulz, S. Zschoche, H.P. Zhang, B. Voit, G. Gerlach, Macroporous smart hydrogels for fast-responsive piezoresistive chemical microsensors, Procedia Eng. 25 (2011) 1141–1144.

[44] Y. Cai, W. Shen, S.L. Loo, W.B. Krantz, R. Wang, A.G. Fane, X. Hu, Towards temperature driven forward osmosis desalination using Semi-IPN hydrogels as reversible draw agents, Water Res. 47 (2013) 3773–3781.

[45] B.A. Getachew, S.-R. Kim, J.-H. Kim, Improved stability of self-healing hydrogel pore-filled membranes with ionic cross-links, J. Membr. Sci. 553 (2018) 1–9.

[46] M.A. Haq, Y. Su, D. Wang, Mechanical properties of PNIPAM based hydrogels: a review, Mater. Sci. Eng. C 70 (2017) 842–855.

[47] S. Chu, M.M. Maples, S.J. Bryant, Cell encapsulation spatially alters crosslink

density of poly(ethylene glycol) hydrogels formed from free-radical polymerizations, Acta Biomater. 109 (2020) 37–50.
[48] Y. Chen, H. Tan, Crosslinked carboxymethylchitosan-g-poly(acrylic acid) copolymer as a novel superabsorbent polymer, Carbohydr. Res. 341 (2006) 887–896.
[49] M.C. Bavya, L. George, R. Srivastava, V. Rohan K, Natural and synthetic materials in regenerative medicine: progress over the past five years, Reference Module in Materials Science and Materials Engineering, 2019.
[50] Y. Hartanto, M. Zargar, X. Cui, Y. Shen, B. Jin, S. Dai, Thermoresponsive cationic copolymer microgels as high performance draw agents in forward osmosis desalination, J. Membr. Sci. 518 (2016) 273–281.
[51] R. Singhal, K. Gupta, A review: tailor-made hydrogel structures (classifications and synthesis parameters), Polym.-Plast. Technol. Eng. 55 (2015) 54–70.
[52] G. Sun, X. Zhang, Z. Bao, X. Lang, Z. Zhou, Y. Li, C. Feng, X. Chen, Reinforcement of thermoplastic chitosan hydrogel using chitin whiskers optimized with response surface methodology, Carbohydr. Polym. 189 (2018) 280–288.
[53] J. Wei, Z.X. Low, R. Ou, G.P. Simon, H. Wang, Hydrogel-polyurethane interpenetrating network material as an advanced draw agent for forward osmosis process, Water Res. 96 (2016) 292–298.
[54] W.A. Laftah, S. Hashim, A.N. Ibrahim, Polymer hydrogels: a review, Polym.-Plast. Technol. Eng. 50 (2011) 1475–1486.
[55] F. Ganji, S. Vasheghani-Farahani, E. Vasheghani-Farahani, Theoretical description of hydrogel swelling: a review, Iran. Polym. J. 19 (2010) 375–398.
[56] K.X. Ma, X.Z. Zhang, Y.Y. Yang, T.S. Chung, Preparation and characterization of fast response macroporous poly(*N*-isopropylacrylamide) hydrogels, Langmuir 17 (2001) 6094–6099.
[57] C. Dima, L. Patrascu, A. Cantaragiu, P. Alexe, S. Dima, The kinetics of the swelling process and the release mechanisms of Coriandrum sativum L. essential oil from chitosan/alginate/inulin microcapsules, Food Chem. 195 (2016) 39–48.
[58] G. Chen, R. Liu, H.K. Shon, Y. Wang, J. Song, X.-M. Li, T. He, Open porous hydrophilic supported thin-film composite forward osmosis membrane via co-casting for treatment of high-salinity wastewater, Desalination 405 (2017) 76–84.
[59] I. Sreedhar, S. Khaitan, R. Gupta, B.M. Reddy, A. Venugopal, An odyssey of process and engineering trends in forward osmosis, Environ. Sci. Water Res. Technol. 4 (2018) 129–168.
[60] Y. Zeng, L. Qiu, K. Wang, J. Yao, D. Li, G.P. Simon, R. Wang, H. Wang, Significantly enhanced water flux in forward osmosis desalination with polymer-graphene composite hydrogels as a draw agent, RSC Adv. 3 (2013) 887–894.
[61] A. Razmjou, Q. Liu, G.P. Simon, H. Wang, Bifunctional Polymer Hydrogel Layers As Forward Osmosis Draw Agents for Continuous Production of Fresh Water Using Solar Energy, Environ. Sci. Technol. 47 (2013) 13160–13166.
[62] Yusak Hartanto, Seonho Yun, Bo Jin, Sheng Dai, Functionalized thermo-responsive microgels for high performance forward osmosis desalination, Water Research A Journal of the International Water Association 70 (2015) 385–393.